Iran J Orthod. 2026 December; 21(2):e1473. doi:10.32592/ijorth.19.1.1473.
Published online 2026 December 1 Research Article
Original Article **Open Access**

A Two-stage Artificial Intelligence Model for Required Space Analysis from Occlusal Photographs: A Diagnostic Accuracy Study

Mostafa Abtahi [1], Yasaman Nakhaei [2], Erfan Bardideh [3], Shadi Nouri [4], Ghazal Asadi [4], Shayan Yousefi [4], Fereshteh Naderi [5]*

[1] Dental Research Center, School of Dentistry, Mashhad University of Medical Sciences, Mashhad, Iran
[2] Resident, Department of Pediatrics, School of Dentistry, Mashhad University of Medical Sciences, Mashhad, Iran
[3] Researcher, Department of Orthodontics, School of Dentistry, Mashhad University of Medical Sciences, Mashhad, Iran
[4] Student Research Committee, School of Dentistry, Mashhad University of Medical Sciences, Mashhad, Iran
[5] Resident, Department of Oral and Maxillofacial Surgery, School of Dentistry, Mashhad University of Medical Sciences, Mashhad, Iran

***Corresponding author:** Fereshteh Naderi

Address: Department of Oral and Maxillofacial Surgery, School of Dentistry, Park Square, Mashhad, Iran

E-mail: fnaderi31@yahoo.com

Received: 2026 September 12; **Revised:** 2026 October 07; **Accepted:** 2026 October 24

Abstract

Aim: Accurate space analysis is fundamental to orthodontic diagnosis, yet conventional cast-based measurement remains time-consuming and operator-dependent. This study aimed to develop and evaluate a two-stage artificial intelligence (AI) workflow for automate tooth-level mesiodistal measurements and required space estimation from standard occlusal photographs.
Methods: This diagnostic accuracy study was based on an initial dataset of 1,428 maxillary and mandibular occlusal photographs from 714 adults, of which 1,424 images were included in the model development and evaluation. You Only Look Once Model (YOLOv8) segmented the dental arch (Stage 1), and a customized Segment Anything Model (SAM) identified tooth landmarks and mesiodistal widths from the second premolar to the contralateral second premolar (Stage 2). Required space was calculated by summing these widths. Blinded manual measurements on plaster casts using a high-precision digital caliper served as the reference standard. Agreement was assessed using intraclass correlation coefficients (ICC), mean absolute error (MAE), BlandAltman analysis, and paired t-tests. P-value<0.05 was considered as significant.
Results: At the individual tooth level, ICCs ranged from 0.84 to 0.92 with MAEs of 0.29–0.48 mm, showing no statistically significant mean bias for the majority of teeth ($P > 0.05$). At the arch level, required space agreement was high, with an ICC of 0.89 (95% CI: 0.88–0.92; MAE: 1.88 ± 0.46 mm; $P = 0.31$) for the maxilla and an ICC of 0.94 (95% CI: 0.92–0.96; MAE: 1.72 ± 0.48 mm; $P = 0.29$) for the mandible.
Conclusion: The proposed two-stage AI workflow demonstrated moderate-to-high agreement with direct cast-based measurements for both individual tooth widths and total required space. While these findings support the technical feasibility of automated image-based required space analysis from routine occlusal photographs, external validation across independent and more diverse clinical populations is necessary before clinical implementation.

Keywords: Artificial Intelligence, Machine Learning, Occlusal Photography, Orthodontic Diagnosis, Space Analysis.

Background

Accurate analysis of the relationship between tooth size and arch dimensions is fundamental to orthodontic diagnosis and treatment planning. A favorable occlusion requires proportional maxillary and mandibular tooth dimensions, and tooth-size discrepancies may compromise the potential to

Copyright © 2026, Author(s). This is an open-access article distributed under the terms of the Creative Commons Attribution-NonCommercial 4.0 International License (http://creativecommons.org/licenses/by-nc/4.0/) which permits copy and redistribute the material just in noncommercial usages, provided the original work is properly cited.

achieve an ideal occlusal relationship. Tooth-size discrepancy is a clinically relevant factor in malocclusion, particularly when mesiodistal widths vary in teeth such as the maxillary lateral incisors or premolars. Space analysis therefore compares the required space, calculated as the sum of the mesiodistal widths of permanent teeth, with the available space in the dental arch. When the required space exceeds the available space, crowding occurs, and when the available space is greater than the required space, spacing is observed (1,2).

The clinical value of space analysis depends on its accuracy and reproducibility. Inadequate diagnostic information, including inaccurate space assessment, may lead to compromised diagnosis, inappropriate treatment planning, unfavorable dental and facial outcomes, and increased risk of relapse. This is particularly important when extraction decisions are considered because such decisions are closely related to the evaluation of tooth size and arch-length relationships. Despite its importance, conventional space analysis remains dependent on manual measurements, operator experience, and clinical judgment. Manual measurement on plaster casts is generally regarded as reliable, but it is time-consuming and can be influenced by technique, calibration, and interpretation (3,4). Studies show that computer-aided or digital model-based space analysis can provide clinically acceptable results, although manual measurements with calibrated gauges have traditionally been considered among the most accurate and repeatable approaches (5,6).

As digital dentistry advances, artificial intelligence (AI) has increasingly been introduced into dental and orthodontic workflows. AI systems can process complex data, learn patterns, and support diagnostic or therapeutic decision-making. In image-based tasks, convolutional neural networks (CNNs) and related deep learning methods have enabled automated object detection, semantic segmentation, and instance segmentation, allowing structures within images to be identified and analyzed at the pixel or object level (7–11). In dentistry, these methods have been applied to diagnostic imaging, prediction, classification, and automated analysis, with the potential to improve efficiency, reduce workload, and support more consistent clinical evaluation (12–14).

Orthodontics is particularly suited to image-based AI because diagnosis commonly relies on photographs, radiographs, and study models. Intraoral photographs are essential diagnostic records and are routinely used for treatment planning, monitoring, communication, and documentation. Occlusal photographs, in particular, provide information about tooth dimensions and arch form. However, manual interpretation of photographic records is time-consuming and may be affected by image quality, visual fatigue, and examiner variability. Recent orthodontic studies have demonstrated the feasibility of using AI for tasks such as assessment of orthodontic treatment need from clinical images, automated classification and archiving of orthodontic photographs, classification of intraoral and facial photographs, and occlusion classification using intraoral photographs (13–16). These findings support AI's potential role as an adjunctive tool in orthodontic diagnosis and treatment planning.

Automated quantitative analysis from standard two-dimensional occlusal photographs remains relatively underexplored. Our team previously reported a two-stage YOLOv8 (You Only Look Once, version 8) – SAM (Segment Anything Model) workflow (16–18) for automated measurement of available arch space using the same parent cohort and five primary arch-perimeter landmarks (19). However, available space and required space represent different measurement targets: available space quantifies the arch perimeter, whereas required space is derived from the mesiodistal widths of the erupted teeth. The present study therefore focuses specifically on automated identification of tooth-level mesial and distal landmarks, measurement of individual mesiodistal tooth widths, and summation of these widths to estimate required space. This study aimed to evaluate agreement between these task-specific measurements and direct cast-based caliper measurements at both the individual tooth and arch levels.

Methods

Study Design

This diagnostic accuracy study is a task-specific analysis within a broader project evaluating artificial intelligence (AI)-based orthodontic space analysis from occlusal photographs, reported in accordance with the STARD-AI guidelines. The study was conducted from 2023 to 2024 at the Department of Orthodontics, School of Dentistry, Mashhad University of Medical Sciences, Iran. The parent cohort comprised 714 adults and 1,428 paired maxillary and mandibular occlusal photographs previously utilized for automated available space measurement (19). Of these, 1,424 images were included in the present model

development and evaluation dataset. (19). The present investigation evaluates a distinct diagnostic outcome: individual mesiodistal tooth widths and their sum as the required space. Previously published available space and overall arch discrepancy results are not re-reported.

The required-space analysis was restricted to the ten teeth extending from the right second premolar to the left second premolar in each dental arch. Third molars (wisdom teeth) were not included in the measurement protocol, and their mesiodistal dimensions did not contribute to the required-space calculations. The first permanent molars were identified only as reference structures for pixel-to-millimeter calibration and were not included in the final required-space summation.

Participant Selection and Eligibility Criteria

A consecutive series of patients meeting the inclusion criteria was selected from both retrospective records and prospective clinical intake. Inclusion criteria required permanent dentition (from the left second premolar to the right second premolar) and available high-quality maxillary and mandibular occlusal photographs. Exclusion criteria were a history of previous or ongoing orthodontic treatment, craniofacial syndromes such as cleft lip and palate, and more than one missing tooth per quadrant. To evaluate the AI model under conditions representative of routine clinical practice, patients with mild-to-moderate congenital dental anomalies (such as localized enamel hypoplasia) were not excluded.

Data Collection

Data were collected using both retrospective and prospective approaches. In the retrospective component, occlusal photographs and patient information were extracted from existing clinical records, provided that corresponding plaster casts were available for the same patients. In the prospective component, occlusal photographs were obtained from new patients under standardized photographic conditions to minimize variations in perspective and illumination. Because the final dataset included images with variations in brightness, angulation, and focal distance, it reflected conditions closer to routine clinical practice and provided a realistic basis for evaluating model performance. Demographic data, including age and sex, were also recorded for each patient.

Reference Measurements

The reference measurements were obtained on plaster casts using a digital caliper. For each plaster cast, the mesiodistal width of each tooth from the left second premolar to the right second premolar was measured by the first author, resulting in 10 tooth-width measurements from the right second premolar to the left second premolar.

Measurements were performed directly on the casts using a digital caliper (Insize Co, Brazil) with an accuracy of 0.01 mm. The sum of these 10 mesiodistal tooth widths was recorded as the reference required space for the corresponding arch. These reference measurements were used to train, validate, and evaluate the accuracy of the AI-based system and to compare automated photographic measurements with conventional manual analysis.

Plaster casts were selected as the reference standard because they were consistently available for both retrospective and prospective records in the study dataset and allowed standardized direct measurement across all included patients. Direct cast-based assessment also allowed physical identification of mesial and distal landmarks without additional image-processing or digital reconstruction steps. Therefore, manual measurements on plaster casts using a high-precision digital caliper served as an appropriate independent reference for evaluating AI-derived measurements from two-dimensional occlusal photographs.

To assess the repeatability of the cast-based reference measurements used in the present required-space analysis, 25 plaster casts were randomly selected and remeasured by the same orthodontic specialist after a two-week interval using the same protocol. Intra-operator agreement was quantified using the intraclass correlation coefficient.

AI Model Design and Implementation

The automated workflow for the required space measurement, which was estimated through tooth width measurement on two-dimensional occlusal images, consisted of two sequential stages: segmentation of the dental arch region using YOLOv8 and landmark-based tooth width estimation using SAM.

The AI-derived required space for each arch was calculated as the sum of the converted mesiodistal widths of 10 teeth, extending from the left second premolar to the right second premolar. For data processing, each occlusal image was assigned to its corresponding patient and arch. The maxillary and mandibular images were analyzed independently. Tooth-level measurements were generated for

each selected tooth, and the arch-level required space was calculated by summing the tooth-level mesiodistal widths.

Stage 1: Segmentation of Occlusal Arches Using YOLOv8

In the first stage, the segmentation version of YOLOV8 (Segmentation version from Ultralytics Inc) was used to separate dental structures, including teeth and gingiva, from non-dental background structures such as the tongue and buccal mucosa. Of the initial 1,428 occlusal photographs obtained from 714 patients, 1,424 images were included in the model dataset. These images were divided into training, validation, and test sets, with 854 images (60%) assigned to training, 142 images (10%) used for validation, and 428 images (30%) reserved for final evaluation. To expand the training dataset, five-fold augmentation was applied by generating four additional modified versions of each original training image. The augmentation process included brightness changes of ±25%, rotation or perspective changes of ±15°, and cropping of ±10%. This yielded approximately 4270 training images, including the original 854 training images and the augmented images, to reduce overfitting and improve model resilience under variable photographic conditions (Figure 1).

The output of the first-stage model was a binary segmentation mask for each occlusal photograph. This mask isolated the dental arch region and removed irrelevant background areas. The resulting masked images were then used as the input for the second stage.

Stage 2: Landmark Detection and Measurement Using SAM

In the second stage, each masked image was processed using the SAM from Meta. The model was customized to identify mesial and distal landmarks of individual teeth from the left first molar to the right first molar, the distal points of the right and left first molars as additional reference landmarks, and the arch midline. Although the first molars were detected by the AI system, they were not included in the reference required space calculation. Their detection was used to support conversion of pixel-based measurements into millimetric values.

For landmark detection, additional advanced augmentation was applied using local distortions of approximately ±5 to ±10 pixels at a five-fold rate. This step was designed to simulate variations related to lens distortion and mirror reflection in intraoral photography and to improve landmark detection under clinical imaging conditions. After landmark identification, the mesiodistal width of each tooth was calculated in pixels as the distance between its mesial and distal landmarks on the occlusal image.

Pixel measurements were converted to millimetric values using a scaling coefficient derived from first molar width. The mean mesiodistal width of the first molars was obtained from a meta-analysis related to Middle Eastern populations, as used in the previous study by Bardideh et al. (16). These reference data were stratified by arch, side, and sex. For each image, the mean pixel width of the right and left first molars on the masked occlusal photograph was compared with the corresponding millimetric first molar width according to sex, arch, and side. This relationship was used to calculate the millimeter-per-pixel conversion factor. The pixel-based mesiodistal widths of the teeth extending from the left second premolar to the right second premolar were then converted to millimeters (Figure 2).

The same procedure was applied separately to the maxillary and mandibular occlusal photographs. Thus, the final automated output for each patient consisted of the required space for the maxillary arch and the mandibular arch.

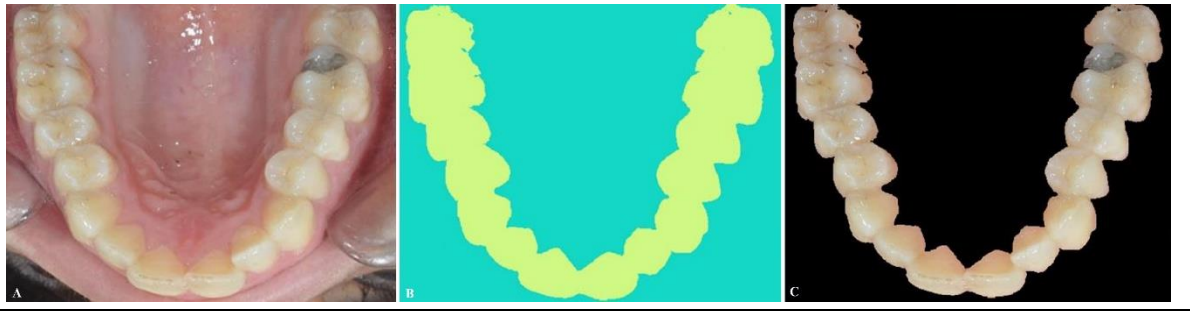


Figure 1. First-stage segmentation of occlusal photographs using YOLOv8. (A) Original occlusal photograph. (B) Binary segmentation mask generated by YOLOv8. (C) Masked occlusal image after removal of non-dental background structures.

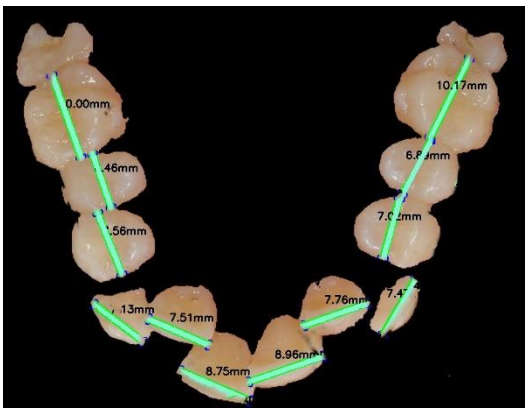


Figure 2. Required-space analysis using the Segment Anything Model (SAM). The masked occlusal image was processed using the customized SAM to identify mesial and distal tooth landmarks and calculate pixel-based mesiodistal tooth widths for required space estimation

Training Space

All model-development codes were implemented in Python 3.8. For the first segmentation stage using YOLOV8 (Segmentation version from Ultralytics Inc), TensorFlow 2.7.0 and Keras 2.8.1 were used, whereas the second-stage SAM was implemented in PyTorch according to the Meta framework. Training was performed on a Linux workstation equipped with an Nvidia A100 graphics processing unit with 48 GB of VRAM and 256 GB of system RAM. The Adam optimizer was used with a batch size of 32 and an initial learning rate of 0.001. Early stopping was applied when validation loss did not improve over 10 consecutive epochs. To reduce the risk of overfitting, five-fold cross-validation was also used during model development.

Relationship to the Previous Available Space Model

The present analysis used the same parent image cohort as the earlier available space study (19). The first-stage YOLOv8 dental arch segmentation component was retrained using the same protocol. The second-stage task was different and was configured/fine-tuned to identify tooth-level mesial and distal landmarks required for mesiodistal width measurement, rather than the five primary arch perimeter landmarks used for available space estimation. Thus, the required space labels, tooth-level measurements, summed required-space outputs, and performance analyses reported here were generated specifically for the present research question.

Statistical Analysis

Statistical analysis was performed using STATA 18 (StataCorp LLC, USA). The normality of measurement differences, defined as the AI-derived value minus the reference cast-based value, was assessed using the Shapiro-Wilk test. Agreement between AI-derived measurements and reference measurements was evaluated at both tooth and arch levels. At the tooth level, the mesiodistal width of each tooth measured by the AI system was compared with the corresponding cast-based reference measurement. At the arch level, the mesiodistal widths of the 10 teeth from the left second premolar to the right second premolar were summed for each arch, and the AI-derived total required space was then compared with the corresponding cast-based reference value. Agreement and lack of systematic bias were assessed using the intraclass correlation coefficient, reported with 95% confidence intervals. Mean absolute error and its standard deviation were also calculated. Bland-Altman analysis was used to estimate mean bias and limits of agreement. Paired t-tests or Wilcoxon's signed-rank tests were used when appropriate, according to the distribution of the measurement differences. Statistical significance was set at $P<0.05$ for all analyses.

Ethical Approval

This study was approved by the Research Ethics Committee of Mashhad University of Medical Sciences, Mashhad, Iran (Ethics approval code: IR.MUMS.DENTISTRY.REC.1402.005). All data were anonymized before analysis and were accessible only to the core investigators.

Results

Dataset Characteristics and Screening

The initial dataset comprised 714 adult patients with permanent dentition, each contributing two standard occlusal photographs (one maxillary and one mandibular), yielding 1,428 images. After excluding four images from the model dataset, 1,424 images were retained for model development and evaluation, including 854 training images, 142 validation images, and 428 test images.

Repeatability of the Reference Standard

Assessment of intra-operator repeatability on 25 randomly selected plaster casts remeasured after a two-week interval demonstrated excellent reliability, with an intraclass correlation coefficient (ICC) of 0.96 (95% CI: 0.94–0.97).

Tooth-level Measurements

At the individual tooth level, the AI-derived mesiodistal tooth widths demonstrated good-to-excellent agreement with the cast-based reference standard. ICC values across individual teeth ranged from 0.84 to 0.92. The mean absolute error (MAE) ranged between 0.29 mm and 0.48 mm, representing approximately 5% to 17% of average tooth width. Although minor systematic differences reached statistical significance for certain anterior teeth (e.g., UL2, $p = 0.04$; LL1, $p = 0.03$), the absolute mean bias remained clinically negligible (≤ 0.05 mm). Detailed tooth-level agreement, error metrics, and mean biases are summarized in Tables 1 and 2.

Arch-level Required Space Analysis

At the arch level, required space was calculated as the cumulative sum of the mesiodistal widths of 10 teeth (from the second premolar to the contralateral second premolar). Agreement between the automated measurements and the cast-based reference was high across both arches, with an ICC of 0.89 (95% CI: 0.88–0.92) for the maxilla and 0.94 (95% CI: 0.92–0.96) for the mandible. The MAE at the arch level was 1.88 ± 0.46 mm for the maxilla and 1.72 ± 0.48 mm for the mandible, corresponding to approximately 2% to 3% of the total arch tooth width. Arch-level agreement and error indices are presented in Table 3.

Table 1. Agreement and measurement error between AI-derived and cast-based mesiodistal tooth-width measurements in the maxillary arch ($\boldsymbol{n = 714}$)

Tooth	ICC (95% CI)	MAE (mm) ± SD	Mean Bias (mm)	*p-value
UL5 (2nd Premolar)	0.92 (0.89–0.94)	0.29 ± 0.10	+0.00	0.63
UL4 (1st Premolar)	0.90 (0.86–0.93)	0.31 ± 0.12	+0.02	0.12
UL3 (Canine)	0.90 (0.86–0.93)	0.34 ± 0.10	+0.03	0.36
UL2 (Lat. Incisor)	0.84 (0.79–0.88)	0.48 ± 0.13	+0.05	0.04
UL1 (Cent. Incisor)	0.86 (0.82–0.90)	0.44 ± 0.14	+0.04	0.07
UR1 (Cent. Incisor)	0.86 (0.82–0.90)	0.42 ± 0.16	+0.02	0.17
UR2 (Lat. Incisor)	0.85 (0.81–0.89)	0.46 ± 0.15	+0.04	0.09
UR3 (Canine)	0.89 (0.85–0.92)	0.35 ± 0.11	−0.01	0.22
UR4 (1st Premolar)	0.91 (0.87–0.94)	0.29 ± 0.12	+0.02	0.14
UR5 (2nd Premolar)	0.92 (0.89–0.94)	0.29 ± 0.10	+0.00	0.63

ICC: Intraclass Correlation Coefficient; MAE: Mean Absolute Error; SD: Standard Deviation.

*Paired t-test comparing AI measurements with cast-based reference.

Table 1. Agreement and measurement error between AI-derived and cast-based mesiodistal tooth-width measurements in the mandibular arch ($\boldsymbol{n = 714}$)

Tooth	ICC (95% CI)	MAE (mm) ± SD	Mean Bias (mm)	*p-value
LL5 (2nd Premolar)	0.91 (0.87–0.94)	0.32 ± 0.11	+0.01	0.18
LL4 (1st Premolar)	0.90 (0.86–0.93)	0.33 ± 0.10	+0.02	0.21
LL3 (Canine)	0.92 (0.88–0.95)	0.36 ± 0.12	−0.01	0.33
LL2 (Lat. Incisor)	0.85 (0.81–0.89)	0.47 ± 0.13	+0.04	0.06
LL1 (Cent. Incisor)	0.84 (0.80–0.88)	0.49 ± 0.14	+0.05	0.03

LR1 (Cent. Incisor)	0.86 (0.82–0.90)	0.45 ± 0.16	+0.02	0.11
LR2 (Lat. Incisor)	0.85 (0.81–0.89)	0.46 ± 0.15	+0.03	0.08
LR3 (Canine)	0.90 (0.86–0.93)	0.34 ± 0.11	+0.01	0.28
LR4 (1st Premolar)	0.88 (0.84–0.92)	0.31 ± 0.12	+0.02	0.17
LR5 (2nd Premolar)	0.91 (0.87–0.94)	0.30 ± 0.11	+0.01	0.24

ICC: Intraclass Correlation Coefficient; MAE: Mean Absolute Error; SD: Standard Deviation.

*Paired t-test comparing AI measurements with cast-based reference.

Table 2. Agreement and measurement error for AI-derived required-space measurements compared with cast-based reference measurements at the arch level ($\boldsymbol{n = 714}$).

Arch	ICC (95% CI)	MAE (mm) ± SD	Mean Bias (mm)	*p-value
Maxilla	0.89 (0.88–0.92)	1.88 ± 0.46	+0.31	0.31
Mandible	0.94 (0.92–0.96)	1.72 ± 0.48	-0.12	0.29

ICC: Intraclass Correlation Coefficient; MAE: Mean Absolute Error; SD: Standard Deviation.

*Paired t-test comparing AI measurements with cast-based reference.

Repeatability of the Cast-based Reference Measurements

Intra-operator repeatability was assessed in 25 randomly selected casts that were remeasured after a two-week interval. The ICC was 0.96 (95% CI: 0.94–0.97), indicating excellent repeatability of the cast-based mesiodistal tooth width/required space reference measurements.

Discussion

This study developed and evaluated a two-stage AI model for estimating required space from occlusal photographs. The combined YOLOv8 and SAM workflow showed high agreement with cast-based reference measurements for both the mesiodistal tooth width and required space estimation. This agreement was consistently high at the individual tooth level and even stronger at the arch level, where the measured required space closely corresponded to the plaster cast reference. Overall, these results support the feasibility of an automated, image-based approach for estimating required space, with good agreement with conventional cast-based measurements.

Accurate space analysis is essential for orthodontic diagnosis and treatment planning, as clinical decisions depend on the relationship between tooth size and arch length. Conventional assessment of required space involves measuring mesiodistal tooth widths on plaster casts, and the diagnostic value of this procedure depends on both precision and reproducibility. Inadequate or inconsistent space analysis may compromise treatment planning, extraction decisions, and the evaluation of crowding or spacing. These findings suggest that an automated system can estimate required space from occlusal photographs with good agreement with conventional cast-based measurements.

This is particularly useful because intraoral photographs are routinely obtained as part of orthodontic records and are easier to store, retrieve, and process than plaster models, which require physical handling and storage.

The model's performance can be understood through the two-stage analytical design. The first stage used YOLOv8 segmentation to isolate the dental arch from surrounding non-dental structures. The second stage used a customized SAM-based workflow to identify mesial and distal landmarks and calculate tooth widths. This separation of background removal from landmark-based measurement was important because occlusal photographs include soft tissues, shadows, mirror reflections, and variations in angulation. By restricting the second-stage analysis to the masked dental arch region, the system reduced irrelevant image information before landmark identification. This approach is consistent with the broader role of deep learning in image analysis, where object detection, semantic segmentation, and instance segmentation allow complex image data to be converted into structured diagnostic outputs (8–11). The relatively high tooth-level ICC values suggested that the system could identify dental landmarks with sufficient consistency across different teeth and arches, despite the variability inherent in clinical photographic records.

The stronger agreement observed at the arch level than at some individual tooth sites was

consistent with the principle of the required space analysis. Required space is calculated by summing the mesiodistal widths of individual teeth rather than relying on a single-tooth measurement. As a result, small deviations in individual tooth measurements may have a limited effect on the overall arch estimate when values are summed across 10 teeth. This may explain the high arch-level ICC values and why the arch-level MAE represented only a small proportion of the total summed tooth width. From a clinical and technical perspective, this distinction is important because the principal target of the system was not only isolated tooth measurement but the estimation of total required space, which forms the basis for identifying space deficiency or excess in the arch.

The findings also align with previous studies showing that digital and computer-assisted methods can approximate conventional orthodontic measurements, although earlier systems were not specifically designed for AI-based required space estimation using occlusal photographs. Schirmer and Wiltshire reported that computer-aided space analysis could be reliable, although they also noted that precise mesiodistal measurements could not always be obtained from reproduced model images and that calibrated manual measurements remained highly accurate (6). The difference between that earlier context and the present study is the use of deep learning-based image segmentation and landmark detection rather than conventional computer-aided measurement from copied dental models. Leifert et al. later showed that digital models could provide clinically acceptable and reproducible space analysis measurements compared with plaster casts (5). The present study extends this digital trend by using standard occlusal photographs rather than three-dimensional digital models, suggesting that image-based AI may provide an alternative route toward automated orthodontic measurements when appropriate reference calibration and image preprocessing are incorporated.

The results also align with the growing use of AI in orthodontic image analysis. Previous studies have reported high diagnostic or classification performance of AI-based systems in orthodontics, including assessment of treatment need, prediction of the need for orthognathic surgery, segmentation of cleft-related maxillary structures, classification of orthodontic images, and automated analysis of facial photographs (14,15,20–23). Talaat et al. reported high accuracy for a YOLO-based algorithm in detecting malocclusion characteristics from intraoral photographs, including crowding or spacing, abnormal overjet or overbite, and crossbite (13). The present study differs from these classification-oriented applications because it addressed a quantitative measurement task. Estimating required space depends on accurately localizing the mesial and distal tooth boundaries and converting pixel-based measurements into millimetric values. Therefore, the high level of agreement observed in this study suggests that AI applied to intraoral photographs may be useful not only for image classification and record archiving, but also for measurement-dependent diagnostic procedures.

The findings should also be considered in relation to a recent study by Bardideh et al., in which an AI system based on intraoral photographs showed strong performance in dental occlusion classification and, in some aspects, outperformed orthodontists; however, its performance in overjet and overbite measurements was not comparable to that of orthodontists (16). This contrast is important because it suggests that the performance of AI systems may vary according to the type of target variable. Occlusion classification from photographs and mesiodistal tooth width measurements on occlusal views may be more suitable for image-based analysis than measurements that depend on three-dimensional depth relationships or sagittal and vertical inter-arch assessments. In the present study, tooth width measurements were performed on occlusal images, where the relevant anatomical landmarks are largely located within the image plane. This may partly explain the favorable agreement with cast-based measurements, particularly when compared with tasks such as overjet and overbite estimation, which are more sensitive to projection error, occlusal relationships, and three-dimensional geometry.

The study also fits within the broader movement toward digital orthodontic records and automated image indexing. Orthodontic diagnosis relies on standardized records, including photographs, radiographs, and casts or digital models. Previous studies have shown that deep learning can classify and archive orthodontic photographs with high accuracy and speed (14,15). Automated required space analysis could complement these systems by adding quantitative diagnostic information to photographic records. This is particularly relevant because image-based workflows may support faster record review, easier archiving, and reduced dependence on physical casts. In settings with limited access to specialist care, such systems may also help standardize preliminary diagnostic assessment, although final

diagnosis and treatment planning must remain under professional supervision.

The present study should also be interpreted in relation to our previously published available space analysis, which used the same 714-patient parent cohort and occlusal image dataset (19). In that study, the second-stage analysis identified five primary landmarks along the arch perimeter to quantify available space. In contrast, the present analysis used tooth-level mesial and distal landmarks to measure the mesiodistal widths of 10 teeth and derived the total required space by summing them up. The additional information provided by the present study is therefore the tooth-specific error/agreement profile and the accuracy of the summed required-space measurement—outcomes that were not reported in the earlier publication. These two analyses complement orthodontic space analysis but address different geometric targets. To avoid duplicate reporting, the previously published overall available-minus-required space comparison with specialist assessment has been omitted from the present manuscript.

The present study's specific contribution is the automated conversion of standard occlusal photographs into tooth-level mesiodistal measurements and a derived required space estimate. This differs from prior AI applications that primarily addressed image classification, diagnostic categorization, cephalometric landmarking, or, in our previous work, available arch space measurements (7,10–16,19–29). By providing quantitative measurements for individual teeth and the summed required space value, the present workflow extends image-based orthodontic AI from arch-level perimeter assessment to tooth-level metric analysis.

Limitations

Several limitations should be considered when interpreting these findings. The study used occlusal photographs obtained under real clinical conditions, and variations in illumination, angulation, mirror reflection, focus, and image quality may have influenced segmentation and landmark detection. Although this variability increased the clinical realism of model evaluation, it may also limit performance in images with severe distortion or inadequate visualization of proximal tooth surfaces. The reference measurements were based on plaster casts, the standard measurement in this study; however, manual cast measurements may still be affected by operator technique, tooth morphology, and landmark identification. The study included adult patients with permanent dentition, and the findings may not directly generalize to mixed dentition, severe tooth anomalies, extensive tooth loss, prior orthodontic treatment, cleft lip and palate, or images with marked distortion. In addition, the system focused on required space estimation from second premolar to second premolar, while complete clinical space analysis also depends on available space assessment, tooth inclination, incisor position, occlusal relationships, and broader treatment objectives. Because the present analysis and the previous available-space study were derived from the same parent cohort, the current findings should not be interpreted as an independent external replication of the earlier model development dataset. Independent external validation in a geographically and clinically distinct cohort remains necessary.

Future studies should evaluate the system using independent external datasets, different age groups, mixed-dentition patients, and more diverse malocclusion patterns. Further refinement of landmark detection, calibration procedures, and integration with available space analysis may support the development of a comprehensive automated orthodontic space analysis tool.

Conclusion

The proposed two-stage AI workflow demonstrated moderate-to-high agreement with direct cast-based measurements for individual mesiodistal tooth widths and estimated required space from standard occlusal photographs. While these preliminary findings suggest that automated image-based required space analysis is technically feasible and may serve as an adjunctive aid in orthodontic screening, further external validation across independent and more diverse clinical populations is necessary before considering any clinical implementation.

Acknowledgments
None.

Conflict of Interests
The authors declare no conflict of interest.

Data Availability
All data analyzed during this study are included in this published article and its supplementary information files. Further details can be obtained from the corresponding author upon reasonable request.

Funding

Vice Chancellor for Research of Mashhad University of Medical Sciences.

Authors' Contributions

Mostafa Abtahi: Conceptualization, Supervision, Validation, Writing review & editing. Yasaman Nakhaei: Investigation, Supervision, Data Curation, Writing review & editing. Erfan Bardideh: Methodology, Investigation, Validation, Software, Writing review & editing. Shadi Nouri: Investigation, Data curation, Formal analysis, Writing review & editing. Ghazal Asadi: Investigation, Formal analysis, Validation,Writing original draft, Writing review & editing. Shayan Yousefi: Methodology, Data curation, Formal analysis, Software, Writing review & editing. Fereshteh Naderi: Project administration, Supervision, Writing review & editing. All authors reviewed and approved the final version of the manuscript and agreed to be accountable for all aspects of the work.

References

1. Hasija N, Bala M, Goyal V. Estimation of tooth size discrepancies among different malocclusion groups. Int J Clin Pediatr Dent. 2014;7(2):82-5. doi: 10.5005/jp-journals-10005-1242.
2. Proffit WR, Fields HW, Larson B, Sarver DM. Contemporary Orthodontics. 6th ed. South Asia ed. India: Elsevier Inc; 2019.
3. Selvaraj M, Sennimalai K. Orthodontic model analysis in the permanent dentition: a review of past and current methods. IP Indian J Orthod Dentofacial Res. 2022;8(4):220-226. doi:10.18231/j.ijodr.2022.038.
4. James RD. A comparative study of facial profiles in extraction and nonextraction treatment. Am J Orthod Dentofacial Orthop. 1998;114(3):265-76. doi: 10.1016/s0889-5406(98)70208-2.
5. Leifert MF, Leifert MM, Efstratiadis SS, Cangialosi TJ. Comparison of space analysis evaluations with digital models and plaster dental casts. Am J Orthod Dentofacial Orthop. 2009;136(1):16.e1-4;. doi: 10.1016/j.ajodo.2008.11.019.
6. Schirmer UR, Wiltshire WA. Manual and computer-aided space analysis: a comparative study. Am J Orthod Dentofacial Orthop. 1997;112(6):676-80. doi: 10.1016/s0889-5406(97)70234-8.
7. Ren R, Luo H, Su C, Yao Y, Liao W. Machine learning in dental, oral and craniofacial imaging: a review of recent progress. PeerJ. 2021;9:e11451. doi: 10.7717/peerj.11451.
8. Yang R, Yu Y. Artificial convolutional neural network in object detection and semantic segmentation for medical imaging analysis. Front Oncol. 2021;11:638182. doi: 10.3389/fonc.2021.638182.
9. Wen T, Tong B, Liu Y, Pan T, Du Y, Chen Y, Zhang S. Review of research on the instance segmentation of cell images. Comput Methods Programs Biomed. 2022;227:107211. doi: 10.1016/j.cmpb.2022.107211.
10. Shan T, Tay FR, Gu L. Application of artificial intelligence in dentistry. J Dent Res. 2021;100(3):232-244. doi: 10.1177/0022034520969115.
11. Schwendicke F, Singh T, Lee JH, Gaudin RA, Chaurasia A, Wiegand T, et al. Artificial intelligence in dental research: checklist for authors, reviewers, readers. J Dent. 2021;107:103610.
12. Anwar SM, Majid M, Qayyum A, Awais M, Alnowami M, Khan MK. Medical image analysis using convolutional neural networks: A Review. J Med Syst. 2018;42(11):226. doi: 10.1007/s10916-018-1088-1.
13. Talaat S, Kaboudan A, Talaat W, Kusnoto B, Sanchez FJ, Elnagar MH, et al. The validity of an artificial intelligence application for assessment of orthodontic treatment need from clinical images. Semin Orthod. 2021;27:164-171. doi:10.1053/j.sodo.2021.05.012
14. Li S, Guo Z, Lin J, Ying S. Artificial intelligence for classifying and archiving orthodontic images. Biomed Res Int. 2022;2022:1473977. doi: 10.1155/2022/1473977.
15. Ryu J, Lee YS, Mo SP, Lim K, Jung SK, Kim TW. Application of deep learning artificial intelligence technique to the classification of clinical orthodontic photos. BMC Oral Health. 2022;22(1):454. doi: 10.1186/s12903-022-02466-x.
16. Bardideh E, Lal Alizadeh F, Amiri M, Ghorbani M. Designing an artificial intelligence system for dental occlusion classification using intraoral photographs: A comparative analysis between artificial intelligence-based and clinical diagnoses. Am J Orthod Dentofacial Orthop. 2024;166(2):125-137. doi: 10.1016/j.ajodo.2024.03.012.
17. Mohammed D, Rahman S, Mutalib S. Dental segmentation via enhanced YOLOv8 and image processing techniques. Mesopotamian J

CyberSecurity. 2024;4:189-202. doi:10.58496/MJCS/2024/022.
18. Villanueva-Miranda I, Rong R, Quan P, Wen Z, Zhan X, Yang DM, Chi Z, Xie Y, Xiao G. Enhancing medical imaging segmentation with GB-SAM: A novel approach to tissue segmentation using granular box prompts. Cancers (Basel). 2024;16(13):2391. doi: 10.3390/cancers16132391.
19. Abtahi M, Yousefi S, Khesali S, Bardideh E, Mansourzadeh M, Salmani N, et al. Designing and developing a two-stage artificial intelligence model for available space analysis in the dental arch: A comparison with manual analysis. APOS Trends Orthod.2026(53): 1. doi: 10.25259/APOS_53_202.
20. Thanathornwong B. Bayesian-based decision support system for assessing the needs for orthodontic treatment. Healthc Inform Res. 2018;24(1):22-28. doi: 10.4258/hir.2018.24.1.22.
21. Shin W, Yeom HG, Lee GH, Yun JP, Jeong SH, Lee JH, Kim HK, Kim BC. Deep learning based prediction of necessity for orthognathic surgery of skeletal malocclusion using cephalogram in Korean individuals. BMC Oral Health. 2021;21(1):130. doi: 10.1186/s12903-021-01513-3.
22. Wang X, Pastewait M, Wu TH, Lian C, Tejera B, Lee YT, Lin FC, Wang L, Shen D, Li S, Ko CC. 3D morphometric quantification of maxillae and defects for patients with unilateral cleft palate via deep learning-based CBCT image auto-segmentation. Orthod Craniofac Res. 2021;24(Suppl 2):108-116. doi: 10.1111/ocr.12482.
23. Soleiman Mezerji M, Sheikhzadeh S, Mirzaie M, Gholinia H. Fully automated orthodontic photograph analysis by machine learning. Caspian J Dent Res. 2023;12(2):70-81. doi: 10.22088/cjdr.12.2.70.
24. Mupparapu M, Wu CW, Chen YC. Artificial intelligence, machine learning, neural networks, and deep learning: Futuristic concepts for new dental diagnosis. Quintessence Int. 2018;49(9):687-688. doi: 10.3290/j.qi.a41107.
25. Schwendicke F, Samek W, Krois J. Artificial intelligence in dentistry: chances and challenges. J Dent Res. 2020;99(7):769-774. doi: 10.1177/0022034520915714.
26. Cejudo JE, Chaurasia A, Feldberg B, Krois J, Schwendicke F. Classification of dental radiographs using deep learning. J Clin Med. 2021;10(7):1496. doi: 10.3390/jcm10071496.
27. 27. Hwang JJ, Jung YH, Cho BH, Heo MS. An overview of deep learning in the field of dentistry. Imaging Sci Dent. 2019;49(1):1-7. doi: 10.5624/isd.2019.49.1.1.
28. Liu J, Zhang C, Shan Z. Application of artificial intelligence in orthodontics: current state and future perspectives. Healthcare (Basel). 2023;11(20):2760. doi: 10.3390/healthcare11202760.
29. Ramasubbu N, Valai Kasim SA, Thavarajah R, Nathamuni Rengarajan K. Applying artificial intelligence to predict the outcome of orthodontic treatment. APOS Trends Orthod. 2024;14(4):264-272. doi:10.25259/APOS_270_2023.